

# Diffusion of Chromium, Manganese, and Iron in $\text{MnCr}_2\text{O}_4$ Spinel

Jolanta Gilewicz-Wolter, Zbigniew Żurek, Joanna Dudala, Jerzy Lis, Marta Homa, and Marcin Wolter

(Submitted July 21, 2005)

As a result of the oxidation of chromium (Cr)-manganese (Mn) steels, a multilayer scale is formed. The intermediate layer of this scale is composed of  $\text{MnCr}_2\text{O}_4$  spinel, and the outer layer is composed of MnO. The aim of the current study is to examine self-diffusion processes in  $\text{MnCr}_2\text{O}_4$  spinel by a tracer method. In experiments, the radioisotopes  $^{54}\text{Mn}$ ,  $^{51}\text{Cr}$ , and  $^{59}\text{Fe}$  were used. The serial sectioning method was applied for the simultaneous evaluation of diffusion rates of Cr, Mn, and iron (Fe) in  $\text{MnCr}_2\text{O}_4$  spinel at 1173 K under a pressure of  $10^5$  Pa in  $\text{SO}_2$  containing 10 Pa  $\text{O}_2$ . This spinel was obtained by a modified sol-gel method from metal nitrates (R. Gajerski and Z. Żurek, personal communication, 14.04.2004). It was found that the dominant mechanism of Mn transport in the studied samples is a volume diffusion, while Cr and Fe are transported mainly through the high-diffusivity paths.

## 1. Introduction

The full description of the mechanism of the oxidation of Cr-Mn steels requires the knowledge of each partial transport process to find out which of them is the slowest and to determine the corrosion rate. It was found that due to the oxidation of these steels in  $\text{SO}_2$ , the thin innermost, fine-grained layer consisting of sulfides and oxides of Mn, Cr, and Fe is formed. The intermediate layer is built mainly of  $\text{MnCr}_2\text{O}_4$  spinel, while MnO is the main component of the outer layer.<sup>[2]</sup>

The aim of this article is to establish the transport processes of Cr, Mn, and Fe in  $\text{MnCr}_2\text{O}_4$  spinel polycrystals, which is one of the scale components. The application of a multitracer method of diffusion measurements in the material mentioned above is presented.

## 2. Experimental Procedure

The  $\text{MnCr}_2\text{O}_4$  spinel was synthesized from Mn and Cr nitrates by a modified sol-gel method. Gel was obtained by the dehydration of molten nitrates at 85 °C, and subsequently the mixture was decomposed at 250 to 300 °C to obtain oxides. The spinel powder was produced by the cal-

ination of powdered oxides at 900 °C in air. To obtain compact samples (pellets 25.4 mm in diameter and 2.5 mm in thickness), the spinel powder was sintered at 1350 °C under 25 MPa in Ar atmosphere. The grain sizes of spinel in pellets are 1 to 3  $\mu\text{m}$  in diameter. Spinel samples were polished to get a flat surface and were degreased with acetone.<sup>[3,4]</sup> Figure 1 shows the cross section of a spinel pellet.

Diffusion experiments were carried out by annealing the samples in a quartz tube in an  $\text{SO}_2$  atmosphere containing 0.01%  $\text{O}_2$  at well-known temperatures (i.e., 1073 and 1173 K). This atmosphere was chosen because our previous corrosion experiments were carried out at the same temperatures and in gas of the same composition. To establish the required defect concentration throughout the specimen, all samples were preannealed at the same temperature and in the same gas that were later used for diffusion annealing. The preannealing time was generally three times longer than the diffusion-annealing time to ensure that the samples were in thermodynamic equilibrium at a given temperature and oxygen partial pressure. The annealing temperature was controlled with an accuracy of  $\pm 3$  K using a Pt-10%Rh thermocouple. The polished and degreased surfaces of the specimens were coated with a carrier-free  $^{54}\text{Mn}$ ,  $^{51}\text{Cr}$ , and  $^{59}\text{Fe}$  chloride solution and were dried under infrared radiation. All of these isotopes emit  $\gamma$  radiation, so the radiation absorption in the specimen material may be neglected. After annealing, the edges of the specimen were cut to eliminate the additional radioactivity originating from the side of the sample. Subsequently, the samples were mounted in polyacrylic resin in steel tubes.

At 1173 K, the diffusion experiments were carried out using two kinds of samples. The first kind was an  $\text{MnCr}_2\text{O}_4$  spinel sample, and the second kind was a spinel sample connected with Cr13Mn18SiCa steel plate (as shown in Fig. 2) to create conditions similar to these that are present during the oxidation of steel when spinel is formed.

The concentration profiles of radioactive  $^{51}\text{Cr}$ ,  $^{54}\text{Mn}$ , and  $^{59}\text{Fe}$  tracers were determined simultaneously by a serial sectioning technique.<sup>[5]</sup> Sections were removed by grinding. The thickness of the removed layer was measured using

---

This article is a revised version of the paper printed in the *Proceedings of the First International Conference on Diffusion in Solids and Liquids - DSL-2005*, Aveiro, Portugal, July 6-8, 2005, Andreas Öchsner, José Grácio and Frédéric Barlat, eds., University of Aveiro, 2005.

---

**Jolanta Gilewicz-Wolter** and **Joanna Dudala**, The Faculty of Physics and Applied Computer Science, AGH University of Science and Technology, Al. Mickiewicza 30, 30-059 Kraków, Poland; **Zbigniew Żurek** and **Marta Homa**, Institute of Inorganic Chemistry and Technology, Cracow University of Technology Warszawska str. 24, 31-155 Kraków, Poland; **Jerzy Lis**, The Faculty of Materials Science and Ceramics, AGH University of Science and Technology, Al. Mickiewicza 30, 30-059 Kraków, Poland; and **Marcin Wolter**, Institute of Nuclear Physics, Polish Academy of Sciences, ul. Radzikowskiego 152, 30-342 Kraków, Poland. Contact e-mail: jwolter@novell.fj.agh.edu.pl.

## Section I: Basic and Applied Research

micrometer sensitivity of about 1  $\mu\text{m}$ . Following the removal of each section, the residual activity of a specimen was counted using a scintillation counter combined with the multichannel analyzer of  $\gamma$  radiation (8200 channels).

### 3. Data Analysis

The duration of diffusional annealing was chosen in such a way that the penetration depth of the tracers was smaller than the thickness of the sample. This allows us to consider the discussed system in terms of approximation to a semi-infinite solid. In polycrystalline  $\text{MnCr}_2\text{O}_4$  specimens, the volume diffusion as well as the diffusion by the high-diffusivity path should be taken into account.

As the residual activity was measured and the self-absorption of  $\gamma$  radiation may be neglected, the counting rate for each isotope after removing the layer of thickness  $x$  is proportional to the contents of the isotope in the remaining sample<sup>[5,6]</sup>:

$$I(x) = A \int_x^\infty c(x') dx' \quad (\text{Eq 1})$$

where  $I$  is the counting rate,  $A$  is the proportionality coefficient,  $x$  is the thickness of the removed layer, and  $c(x')$  is the isotope concentration.

The volume diffusion is described by Fick's second law:

$$c(x, t) = \text{const} \cdot \exp\left(\frac{-x^2}{4D_T^* t}\right) \quad (\text{Eq 2})$$

where  $D_T^*$  is the tracer diffusion coefficient and  $t$  is the duration of the diffusion process. The diffusion through the grain boundaries occurs in parallel. This process is described by the Whipple-Le Claire equation<sup>[7]</sup>:

$$s\delta D_T^{\text{gb}} = 0.3292 \cdot \left(D_T^*/t\right)^{1/2} \cdot \left[-\partial \ln c(x, t) / \partial x^{6/5}\right]^{-5/3} \quad (\text{Eq 3})$$

where  $s$  is a segregation coefficient,  $\delta$  is a width of the grain boundaries, and  $D_T^{\text{gb}}$  is the diffusion coefficient of the grain boundaries.

The numerically integrated function is fitted to the measured counting rates at different thicknesses of the removed material. In the fitting procedure, the following function is used:

$$I(x, t) \approx \int_x^\infty dx' \cdot \left\{ A_0 \cdot \exp(-x'^2/4D_T^* t) + A_1 \cdot \exp\left[-(0.3292 \sqrt{D_T^*/t})^{3/5} \cdot \left(\frac{x'^2}{s\delta D_T^{\text{gb}}}\right)^{3/5}\right] \right\} \quad (\text{Eq 4})$$

where  $A_0$  and  $A_1$  are constants. The first part of Eq 4 de-

**Table 1** Tracer volume and grain boundary diffusion coefficients of  $^{51}\text{Cr}$ ,  $^{54}\text{Mn}$ , and  $^{59}\text{Fe}$  in  $\text{MnCr}_2\text{O}_4$

Radioisotopes	1073 K spinel		1173 K spinel		1173 K steel-spinel system	
	$D_T^*$ , $\text{cm}^2/\text{s}$	$s\delta D_T^{\text{gb}}$ , $\text{cm}^3/\text{s}$	$D_T^*$ , $\text{cm}^2/\text{s}$	$s\delta D_T^{\text{gb}}$ , $\text{cm}^3/\text{s}$	$D_T^*$ , $\text{cm}^2/\text{s}$	$s\delta D_T^{\text{gb}}$ , $\text{cm}^3/\text{s}$
$^{51}\text{Cr}$	$(9.7 \pm 1.3) \times 10^{-13}$	$(7.6 \pm 3.6) \times 10^{-15}$	$(7.2 \pm 3.5) \times 10^{-11}$	$(2.2 \pm 0.9) \times 10^{-13}$	$(5.5 \pm 0.8) \times 10^{-11}$	$(2.5 \pm 0.5) \times 10^{-13}$
$^{54}\text{Mn}$	$(1.7 \pm 1.4) \times 10^{-12}$	$(1.1 \pm 0.2) \times 10^{-14}$	$(2.9 \pm 0.2) \times 10^{-10}$	...	$(22 \pm 0.5) \times 10^{-11}$	...
$^{59}\text{Fe}$	$(1.2 \pm 0.6) \times 10^{-12}$	$(2.6 \pm 1.0) \times 10^{-15}$	$(4.8 \pm 0.7) \times 10^{-12}$	$(2.5 \pm 1.3) \times 10^{-11}$	$(29 \pm 0.7) \times 10^{-11}$	...

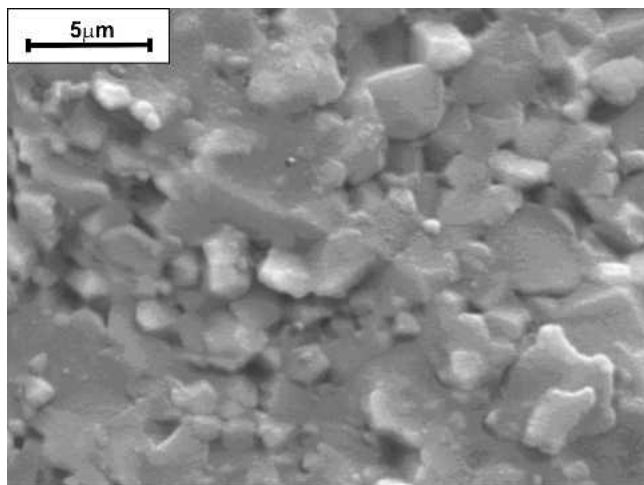


**Fig. 1** The cross section of the spinel  $\text{MnCr}_2\text{O}_4$  pellet

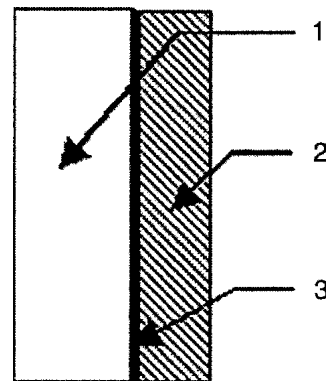
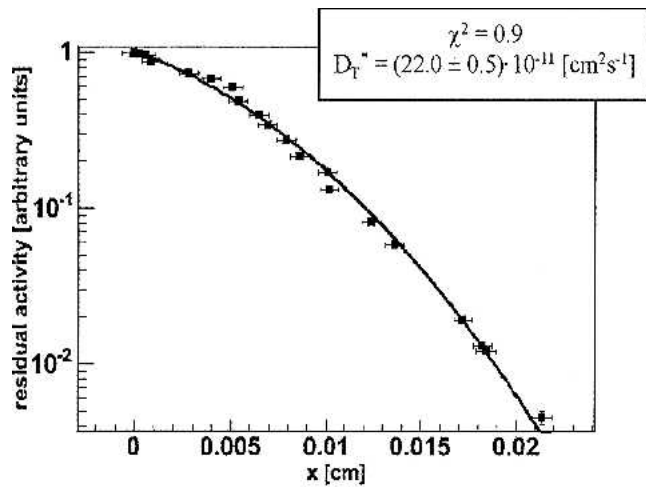
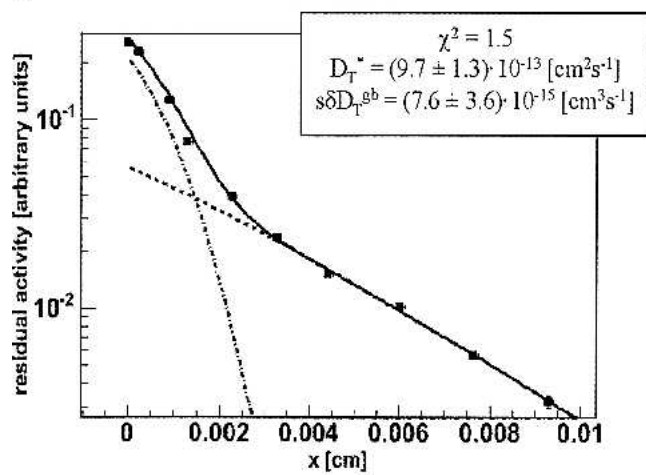


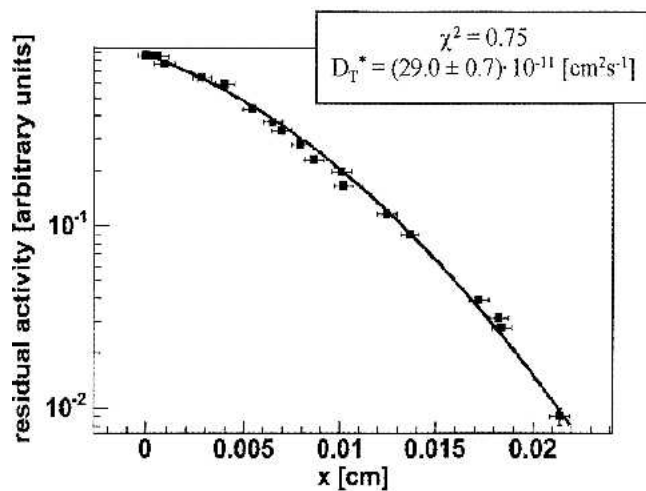
**Fig. 2** The scheme of the connection of the spinel sample with the plate of the  $\text{Cr}_{13}\text{Mn}_{18}\text{SiCa}$  steel: 1, steel; 2, spinel sample; 3, thin layer of radioisotopes



(a)



(b)



(c)

Fig. 3 Residual activity versus  $x$  of (a)  $^{54}\text{Mn}$  in a spinel-steel system at 1173 K, (b)  $^{51}\text{Cr}$  in the spinel at 1073 K, and (c)  $^{59}\text{Fe}$  in a spinel-steel system at 1173 K

describes the volume diffusion, while the second part describes the diffusion by the high-diffusivity path. Because both the thickness of the removed layer and the activity

Table 2 Comparison of estimated distances passed by tracers during the annealing time  $t$  in spinel and spinel-steel system

Measurement	Spinel	Spinel	Spinel-steel
Annealing time, min	10,082		2053
Temperature, K	1073		1173
Range, cm			
$^{51}\text{Cr}$	0.010	0.025	0.021
$^{54}\text{Mn}$	0.017	0.030	0.021
$^{59}\text{Fe}$	0.008	0.018	0.020

have measurement uncertainties, the  $\chi^2$  value is computed as the sum of the quantity below at each point:

$$\chi^2 = \frac{[y - f(x)]^2}{\partial y^2 + \left[ \frac{f(x + \partial x) - f(x - \partial x)}{2} \right]^2} \quad (\text{Eq 5})$$

where  $x$  and  $y$  are the point coordinates, and  $\partial x$  and  $\partial y$  are their errors.

The above-described method of data analysis was applied, because in the “differential” method (Eq 6) the spread of points is artificially increased by dividing the small  $\Delta I$  by the small  $\Delta x$ . Also the neighbor points are correlated, because the same data points are used to calculate them.

$$\frac{dI}{dx} = C \exp\left(-\frac{x^2}{4D_T^*t}\right) \quad (\text{Eq 6})$$

where  $C$  is constant. The “integral” method allows the proper calculation of the uncertainty because the data points are uncorrelated in contrast to the calculation used in the differential method.

#### 4. Results and Discussion

As was mentioned, the scale that forms on Cr-Mn steels in  $\text{SO}_2$  at  $10^5$  Pa is composed of an intermediate layer containing  $\text{MnCr}_2\text{O}_4$  spinel and an outer layer of  $\text{MnO}$ . The rate of oxidation is controlled by the outward diffusion of metals.

It has been shown that over the major part of the phase field, corresponding to higher oxygen activities,  $\text{MnO}$  and  $\text{Cr}_2\text{O}_3$  oxides are the metal-deficit p-type semiconductors with the predominant defects being cation vacancies and electron holes. The self-diffusion coefficient of Mn in  $\text{MnO}$  at 1173 K and 10 Pa  $\text{O}_2$  is on order of  $10^{-9}$   $\text{cm}^2/\text{s}$ ,<sup>[81]</sup> whereas that for Cr in  $\text{Cr}_2\text{O}_3$  is on the order of  $10^{-15}$   $\text{cm}^2/\text{s}$ .<sup>[91]</sup> The defect concentration in such oxides depends on the oxygen activity. All experiments presented in this article were performed in conditions of constant oxygen activity (in  $\text{SO}_2$  at  $10^5$  Pa containing  $10^{-2}$   $\text{O}_2$ ). The calculated diffusion coefficients are listed in Table 1. Figure 3 shows the examples of plots of residual activity versus distance  $x$ . At 1173 K, in

## Section I: Basic and Applied Research

both the spinel and the spinel-steel system, the dominant  $^{54}\text{Mn}$  transport process is volume diffusion, while this is the case for  $^{59}\text{Fe}$  diffusion in the spinel-steel system only. The rate of volume diffusion of  $^{54}\text{Mn}$  in the spinel and the spinel-steel system is the highest one (Table 1). The diffusion to the metal phase was not observed in these conditions. In the case of Cr, high-diffusivity path diffusion is also observed at this temperature. At 1073 K, volume and high-diffusivity path diffusion were found for all of the studied metals.

The Mn diffusion coefficient in the  $\text{MnCr}_2\text{O}_4$  spinel is one order of magnitude less than that for MnO. On the basis of our results, it is difficult to determine the rate of transport of which of the metals is the greatest. However, for the corrosion description it is important which metal may reach the outermost surface and react with the oxidant. Therefore, for example, the values for particular distances passed by tracers during the annealing time  $t$  in the  $\text{MnCr}_2\text{O}_4$  spinel are listed in Table 2. The mechanism of this transport (i.e., bulk or grain-boundary diffusion) is not so important.

### 5. Conclusions

On the basis of the presented results, several conclusions can be drawn:

- At 1173 K, the dominant transport process of Mn in  $\text{MnCr}_2\text{O}_4$  is volume diffusion, whereas for Cr and Fe grain boundary diffusion was additionally observed.
- At 1073 K for all of the studied metals, both mechanisms, bulk and grain-boundary diffusion, were found.
- In the case of the steel-spinel system, the bulk diffusion

coefficient for Fe is about one order of magnitude higher than that in the spinel sample, and only bulk diffusion was observed.

### Acknowledgment

This research was supported by the grant No 3 T08C 055 26 from the Ministry of Science Research and Information Technology, Poland.

### References

1. R. Gajerski and Z. Żurek, private communication, 14.04.2004
2. Z. Żurek, J. Gilewicz-Wolter, M. Hetmańczyk, J. Dudała, and A. Stawiarski, High Temperature Corrosion of Chromium-Manganese Steels in Sulfur Dioxide, *Oxid. Metals*, in press
3. S.H. Song and Z.X. Yuan, Electrical Properties of  $\text{MnCr}_2\text{O}_4$  Spinel, *J. Mater. Sci. Lett.*, Vol 22, 2003, p 755-757
4. P. Papaicovou, H.J. Grabke, M. Danielewski, and H.P. Schmidt, Conversion of Manganese-Chromium Spinel to Sulphides in  $\text{H}_2$ - $\text{H}_2\text{O}$ - $\text{H}_2\text{S}$  Atmospheres, *React. Solids*, Vol 8, 1990, p 147-158
5. S.J. Rothman, *The Measurements of Tracer Diffusion Coefficients in Solids, Diffusion in Crystalline Solids*, G.E. Murch and A.S. Nowicki, Ed., Academic Press, New York, 1984
6. J. Gilewicz-Wolter and M. Wolter, Tracer Diffusion of Iron in  $\alpha$ - $\text{Mn}_{1+y}\text{S}$  Polycrystals, *Solid State Commun.*, Vol 117, 2001, p 719-722
7. I. Kaur and W. Gust, *Fundamentals of Grain and Interphase Boundary Diffusion*, Ziegler Press, Stuttgart, 1988
8. N.L. Peterson and W.K. Chen, Cation Self-Diffusion and the Isotope Effect in  $\text{Mn}_{1-\delta}\text{O}$ , *J. Phys. Chem. Solids*, Vol 43, 1982, p 29-38
9. P. Kofstad, *High Temperature Corrosion*, Elsevier Applied Science, London and New York, 1988